Journal of the Indian Chemical Society 98 (2021) 100177

Contents lists available at ScienceDirect

Journal of the Indian Chemical Society

journal homepage: www.editorialmanager.com/JINCS/default.aspx

Synthesis, characterization, and application of hollow ceramic microsphere based Pd catalyst for hydrogenation of 2-ethylanthraquinone

Anjali A. Ingle, Diwakar Z. Shende, Kailas L. Wasewar *

Advanced Separation and Analytical Laboratory (ASAL), Department of Chemical Engineering, Visvesvaraya National Institute of Technology, Nagpur, 440010, Maharashtra, India

ARTICLE INFO

Keywords:
2-Ethylanthraquinone
Hollow ceramic microspheres
Palladium catalyst

ABSTRACT

Palladium metal has been used extensively in the hydrogenation reactions due to their great affinity towards hydrogen atoms. In the present study, the catalyst preparation attempted with Pd supported Hollow Ceramic Microspheres using wet impregnation method and its use as catalysts is explored in the hydrogenation of 2-ethylanthraquinone studing the effect of the reaction time, temperature, volume of working solution and the catalyst dosages on the conversion of 2-ethylanthraquinone and yield of hydrogen peroxide. The hydrogenation reaction of 2-ethylanthraquinone is the key step in the anthraquinone method for the industrial production of the hydrogen peroxide. The Pd supported catalyst was characterized by XRF, FTIR, and BET to confirm the composition of the prepared catalyst, Pd deposition, and the surface area. The highest catalyst activity was found to be 9.42 g/L with the maximum conversion of 96% at 70°C, 0.3 MPa. The kinetics of the heterogeneous hydrogenation reaction of 2-ethylanthraquinone with Pd supported on Hollow Ceramic Microspheres as catalyst was also investigated. This paper is in contribution of our earlier publication.

1. Introduction

Hydrogen peroxide (H_2O_2) can be termed as green oxidant as it doesn't generate any polluting compound except water and oxygen. It is generally used in the chemical and environmental industries. The market of H_2O_2 is primarily depended on the anthraquinone oxidation (AO) process, in which the anthraquinone derivative typically 2-ethylanthraquinone (EAQ), hydrogen and oxygen are mixed with desired organic solvent and reacted simultaneously to produce H_2O_2 [1]. Subsequently, H_2O_2 is extracted and concentrated in the aqueous phase due to its solubility in water [2,3].

The use of catalyst for the hydrogenation of EAQ is an important parameter in the production of H_2O_2 with AO process. Riedl et al. (1939) invented the first commercial production of H_2O_2using the hydrogenation of EAQ which consists of conversion of EAQ into EAHQ in a slurry reactor using Raney nickel catalyst [4]. They used the working solution as a mixture of two organic solvents namely benzene and secondary alcohols C7-Cll. In the recent time, Palladium (Pd) supported catalysts are considered preferably due to their higher activity and selectivity in the EAQ hydrogenation [5,6]. Al_2O_3, SiO_2, and SiO_2–Al_2O_3 are commonly used as supports for the Pd catalyst. The process development of the existing catalyst system for the hydrogenation of EAQ needs necessary modifications in the supporting materials for the catalyst [7–13]. The rigorous efforts have been attempted in the field of process development for the hydrogenation step, but the reaction kinetics and the order of the reaction need to be studied. Hence, it is important to design a catalyst for the hydrogenation of EAQ which can lower the mass transfer resistance. Drelinkiewicz [14] developed a mathematical model for the catalytic hydrogenation of a mixture of the EAQ using Raney nickel catalyst [14]. The overall reaction rate was the rate controlling step for mass transfer resistance [15,16]. It was observed that the hydrogenation of EAQ follows zero order reaction with respect to EAQ concentration [17].

It is highly preferable to enhance the existing catalyst and modify its structure for the improvement in the hydrogenation of EAQ. Catalysts are pre-impregnated using Pd metal ions on various types of support such as C, Al_2O_3, ZrO_2, and SiO_2 for the fast reaction [18]. The Ni–B on SBA-15 by reluctant impregnation, Cr modified nanosized amorphous Ni–B by chemical reduction, Pd on PAN (SiO_2) composite by oxidative polymerization deposition, Pd on ZrO_2-γ-Al_2O_3 by impregnation, Pd on porous glass beads by subcritical water treatment and ion exchange, Pd on raschig ring alumina by wet impregnation, Pd on Al_2O_3 by oil drop and impregnation and Pd on γ-Al_2O_3 by adsorption-reduction supported catalysts have been reported for the hydrogenation of EAQ in the available literature [19–25]. Supported Pd catalysts are mostly used in the AQ

* Corresponding author.
E-mail addresses: k_wasewar@rediffmail.com, klwasewar@che.vnit.ac.in (K.L. Wasewar).

https://doi.org/10.1016/j.jics.2021.100177
Received 29 January 2021; Received in revised form 21 September 2021; Accepted 22 September 2021

process for the catalytic hydrogenation of the EAQ due to their high selectivity as catalyst and easy removal from the working solution.

In the present study, the Hollow Ceramic Microspheres (HCMs) was employed as Pd support to synthesize Pd/HCM catalyst. The characterization of catalyst was performed with BET surface area analyzer, X-ray Fluorescence Spectrometer (XRF), and Fourier Transform Infrared Spectrometer (FTIR) were used to examine the catalytic activity of the prepared catalyst. The hydrogenation of 2-ehtylanthraquinone for the production of hydrogen peroxide has been intensively investigated using the synthesized catalyst.

2. Materials and methods

2.1. Chemicals

2-Ethyl-9,10-anthraquinone (EAQ, Alfa Asar, purity > 99.0%), HPLC grade water (Merck), palladium chloride ($PdCl_2$, Sigma Aldrich, purity > 99.9%), anhydrous methanol (HPLC grade, Merck, purity > 99.9%), concentrated sulphuric acid (SD Fine-Chem. Ltd., purity > 98.0%), ethanol (Merck, purity > 99.9%), mesitylene (Loba, purity > 98.0%), trioctyl phosphate (TOP, Alfa Asar, purity > 96.0%), xylene (SD Fine-Chem. Ltd., purity > 99.0%), concentrated nitric acid (SD Fine-Chem. Ltd., purity > 99.9%), and potassium permanganate (SD Fine-Chem. Ltd., purity > 98.0%) were purchased as analytical grade and used without any further purification. HCMs, also known as Cenosphere is a lightweight, inert and hollow sphere made up of silica and alumina. HCMs with a size ranging from 5 to 500 μm with the typical composition of 50–65% Al_2O_3, 20–36% SiO_2, and 2–10% Fe_2O_3. HCM was supplied by M/S Vipra Ferro Alloys Pvt. Ltd., Nagpur, Maharashtra, India.

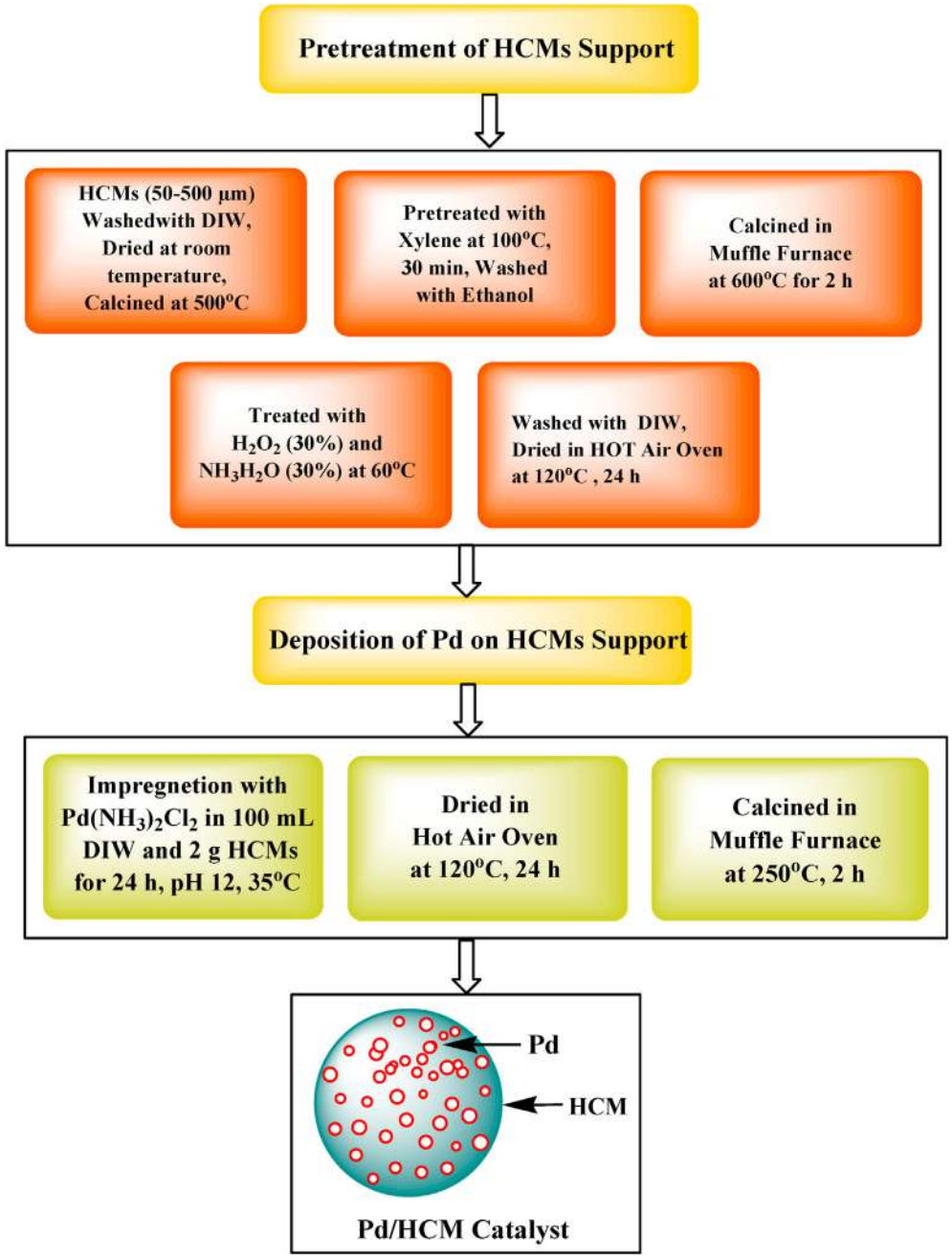

Fig. 1. Schematic representation of various steps in synthesis of Pd/HCM catalyst.

2.2. Pre-treatment of HCMs

The HCMs were selected as catalyst support and studied its applications for the Pd catalyst. HCMs, was harvested using the appropriate techniques. After that, it was subjected to treatment of concentrated nitric acid (HNO_3). Stirring the slurry for 1 h. The slurry was then washed several times with distilled water before being filtered and dried to obtain the treated HCMs. The treated HCMs were calcined at 500°C. The calcined HCM as support was immersed in xylene for 30 min at 100°C. Further the support was thoroughly washed with ethanol and calcined at 600°C for 2 h in a muffle furnace to eliminate the residual xylene. The pre-treated support was washed with H_2O_2 (30%) and NH_3H_2O (30%) simultaneously. Finally, the support was washed with deionized water and dried in hot air oven at 120°C for 24 h.

2.3. Deposition of Pd on pre-treated HCMs

A wet impregnation technique using $PdCl_2$ as a Pd metal precursor assisted the Pd on HCM. In 100 mL of deionized water, 42 mg of $PdCl_2$ was dissolved, and added 2 g HCMs to the resulting solution. 30% aqueous ammonia was added dropwiseto maintain the pH at 12. The resulting $PdCl_2$ and HCMs mixture was stirred at room temperature for 24 h. The impregnation of Pd on the surface of HCMs causing it to settle down at the bottom. The impregnated HCMs was thoroughly washed with deionized water to extract Cl^- ions after complete evaporation of excess water, then dried at 110°C for 6 h. The sample of PdO/HCM was obtained by calcination of the dried product for 2 h in air at 350°C in a muffle furnace. Thus, Pd/HCM catalyst was prepared by reducing PdO/HCM catalyst in presence of the H_2 (0.3 MPa) at 200°C for 2 h. Fig. 1 depicts a schematic representation of the Pd/HCM catalyst preparation.

2.4. Hydrogenation of EAQ

The catalytic activity was tested in the high-pressure autoclave reactor of 50 mL (Amar Equipments, India). The schematic representation of the experimental setup has been shown in Fig. 2. The hydrogenation reaction was performed at 75°C, 0.3 MPa, and 1000 rpm. The EAQ (109 g/L) working solution was prepared as a mixture of EAQ, nonpolar solvent mesitylene, and polar solvent trioctylphosphate with a 1:1 volume ratio. 30 mL of EAQ working solution and reduced catalyst (Pd/HCM) were put together into the autoclave with continuous stirring. Initially, nitrogen was fed into the reactor to remove air. After sealing the reactor, the autoclave was heated to 75°C and after the temperature stabilized the reaction was started quickly by replacing the gas phase with hydrogen. To eliminate the possibility of external mass-transfer limitations, preliminary experiments were performed using varying stirring speeds (in the range of 500–1500 rpm). The results showed that conversion was constant when the stirring speed was 1000 rpm. Thus, the stirring speed was set at 1000 rpm for all the experiments in this study. The entire 30 mL of solution was instantly transferred to a centrifuge to separate the solid catalyst at 4000 rpm for 5 min after finishing the hydrogenation reaction. Then 2 mL of solution with no catalyst inside was transferred into 20 mL of deionized water and oxidized for 20 min with pure oxygen at atmospheric pressure and ambient temperature. It can be judged the completion of oxidization by observing the color of the solution. The concentration of H_2O_2 was determined by titration with $KMnO_4$ solution. In the titration, 5 mL of H_2SO_4 (20 wt.%) solution was mixed with 2 mL of H_2O_2 (aqueous) solution before titration with the $KMnO_4$ solution. In the previous studies, the resulting solution was extracted twice with distilled water and then titrated with the $KMnO_4$ solution to determine the concentration of H_2O_2 [26–31].

The high-performance liquid chromatography (HPLC) was carried out using Agilent1200, USA with DAD detector (254 nm), equipped with a Zorbax C18 column to analyze the concentration of EAQ in the organic phase using 80% methanol and 20% HPLC water as a mobile phase. The well-defined peak of standard EAQ was established at the retention time of about 9.5 min.

2.5. Determination of kinetic parameters

The hydrogenation reaction of EAQ is depicted in Fig. 3. The rate of hydrogenation reaction for the decomposition of EAQ and H_2 was investigated by calculating the moles of EAQ and H_2 reacted per unit time. During the experiments, the reaction was carried out at 1000 rpm, 75°C, and 0.3 MPa. At the high stirring rate, the agitation does not affect the rate of consumption of EAQ and H_2. The overall rate expression in terms of both reactants can be written as [32]:

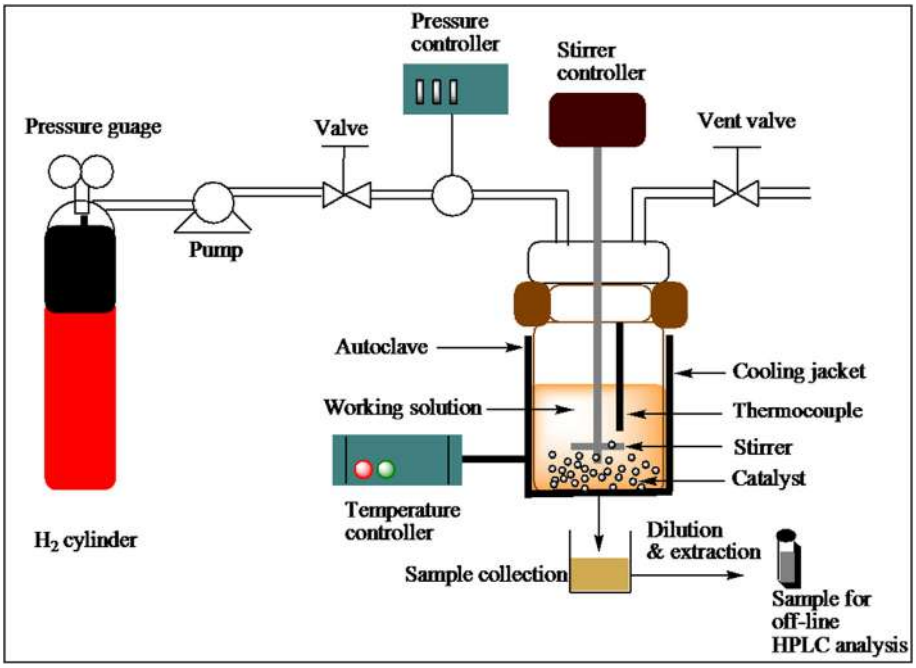

Fig. 2. Catalytic hydrogenation of EAQ in high pressure autoclave reactor.

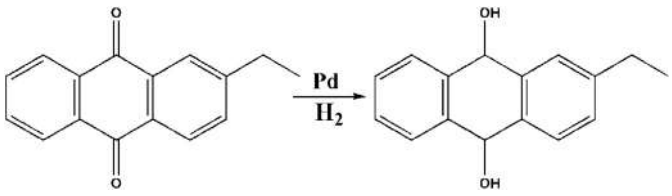

Fig. 3. Hydrogenation reaction of EAQ using Pd based catalyst.

$$-r = k_{mn}(C_{EAQ})^m (C_{H_2})^n \tag{1}$$

Where, $C_{H_2} = \frac{P_{H_2}}{RT}$.

For the first-order kinetics in the stirred tank slurry reactor, the gaseous reactant is bubbled through a liquid reactant consisting of suspended particles of the catalyst. The reaction is occurring at the surface of the catalyst particles, hence the gaseous reactant has to diffuse through the liquid film to the bulk of the liquid and then the film surrounding the catalyst particle as shown in Fig. 4. The rate of reaction at catalyst surface can be equated to the rate of mass transfer through each of the films as follows [33]:

$$r = r_1 = r_2 = r_3 = r_4 \tag{2}$$

$$r_1 = k_g a_{gl}[(P_{H_2} - P_{H_{2i}}) / H_r] \tag{3}$$

$$r_2 = k_{gl} a_{gl}(C_{H_{2i}} - C_{H_2}) = k_{gl} a_{gl}(P_{H_{2i}} - P_{H_2}) / H_r \tag{4}$$

$$r_3 = k_{ls} a_s (C_{H_2} - C_S) = k_{ls} a_s (P_{H_2} - P_S) / H_r \tag{5}$$

Where, r_1, r_2, r_3, and r_4 are the rate of mass transfer through gas film, gas-liquid interface, liquid-solid interface, and at the surface of the catalyst particle. k_g, k_{gl}, and k_{ls} are the gas, gas-liquid, and liquid-solid mass transfer coefficient in m/s. a_{gl} and a_s are the interfacial area for gas-liquid interface and catalyst particle in m^2/m^3.

The rate of reaction at the surface of the catalyst particle can be given as follow:

$$r_4 = k a_s C_S = k a_s P_S \left(\frac{1}{H_r}\right) \tag{6}$$

Where k is the first-order rate constant for the surface reaction. On

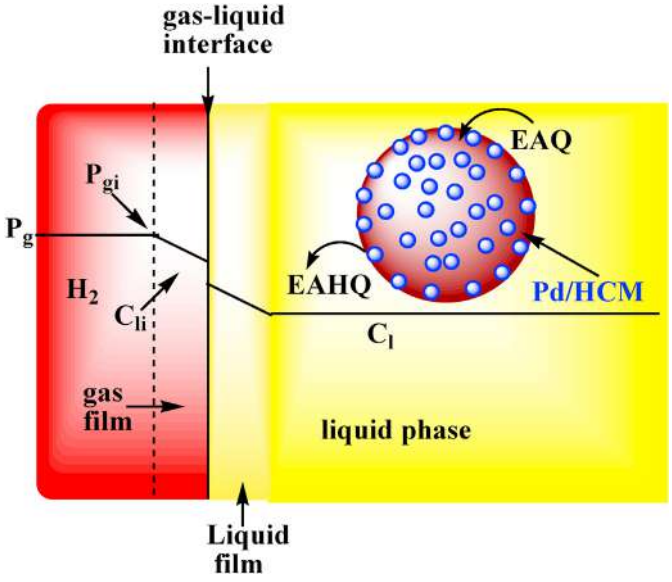

Fig. 4. Schematic representation of concentration profile of H_2 gas.

combining equations (3)–(5), and (6) at the steady-state condition, the rate of reactions can be given with eliminating C_S and C_l as:

$$r = \frac{P_{H_2}}{\left[\left(\frac{1}{k_g a_{gl}} + \frac{1}{k_{gl} a_{gl}} + \frac{1}{k_{ls} a_s} + \frac{1}{k a_s}\right) H_r\right]} \tag{7}$$

Since H_2 is pure gas and diffuses rapidly through gas film, the gas film resistance can be negligible. Hence, the rate of reaction can be written as:

$$r = \frac{P_{H_2}}{\left[\left(\frac{1}{k_{gl} a_{gl}} + \frac{1}{k_{ls} a_s} + \frac{1}{k a_s}\right) H_r\right]} \tag{8}$$

On rearranging equation (8);

$$\frac{P_{H_2}}{r} = \left(\frac{H_r}{k_{gl}}\right)\left(\frac{1}{a_{gl}}\right) + \left(\frac{H_r}{k_{ls}} + \frac{H_r}{k}\right)\left(\frac{1}{a_s}\right) = \frac{C_1}{a_{gl}} + \frac{C_2}{a_s} \tag{9}$$

Where, $C_1 = \frac{H_r}{[k_{gl}]}$ and $C_2 = \left(\frac{H_r}{k_{ls}} + \frac{H_r}{k}\right)$. The effect of varying the stirring was studied with constant temperature, pressure, and the catalyst doses.

Agitation enhances the mass transfer by decreasing the bubble size, leading to increasein the gas-liquid interfacial area and decrease the thickness of the liquid films surrounding the H_2 bubbles and catalyst particles. The effect of specific surface area provided by the catalyst (a_s) was studied at constant temperature, pressure, and the stirring speed using various catalyst doses. The specific surface area of catalyst can be calculated as:

$$a_s = m_s \left(\frac{6}{d_p}\right)\left(\frac{\rho_l}{\rho_p}\right) \tag{10}$$

Where m_s is the catalyst loading in (kg/m^3); a_s, the specific surface area of the catalyst (m^2/m^3); d_p, diameter of the catalyst particle (m); ρ_p, density of the catalyst (kg/m^3); and ρ_l, the density of EAQ (kg/m^3). The rate of reaction can be rewritten using equations (9) and (10) as follows:

$$\frac{1}{r} = C_1' + \frac{C_2'}{m_s} \tag{11}$$

Where, $C_1' = \frac{H_r}{[k_{gl} a_{gl} P_{H_2}]}$ and $C_2' = \frac{\left(\frac{H_r}{k_{ls}} + \frac{H_r}{k}\right)}{\left[P_{H_2}\left(\frac{6}{d_p}\right)\left(\frac{\rho_l}{\rho_p}\right)\right]}$ which can be used to evaluate the resistance for the gas-liquid interface, the product of the mass transfer coefficient, and gas-liquid interfacial area as $\frac{1}{k_{gl} a_{gl}}$ and the combined reaction resistance as $\left[\frac{1}{k_{ls}} + \frac{1}{k}\right]$.

The conversion of EAQ (x), the yield of H_2O_2 (y), hydrogenation efficiency (B), and selectivity of EAQ (S) were calculated using equations (12)–(15) [23,25,34]:

$$x_{EAQ}(\%) = \frac{n_{0(EAQ)} - n_{(EAQ)}}{n_{0(EAQ)}} \times 100 \tag{12}$$

$$y_{H_2O_2}(\%) = \frac{n_{(H_2O_2)}}{n_{0(EAQ)}} \times 100 \tag{13}$$

$$B\left(g/L\right) = \frac{5 C_{KMnO_4} \times V_{KMnO_4} \times M_{H_2O_2}}{2V} \tag{14}$$

$$S(\%) = \frac{n_{(EAQ)} + n_{(H_2O_2)}}{n_{0(EAQ)}} \times 100 \tag{15}$$

3. Results and discussion

3.1. Characterization of catalyst

The elemental analysis or trace element analysis to evaluate the composition of the prepared catalyst was performed by the X-ray Fluorescence Spectrometer (XRF) (Malvern Panalytical Epsilon 3XLE). The XRF spectrometer elemental analysis ranging from carbon (C) to americium (Am) and the concentration range from sub-ppm to 100 wt.%. The composition of HCMs and Pd/HCM are presented in Table 1. Both the materials; support and the catalyst contain Al_2O_3 and SiO_2 in significant proportion and other compounds Fe_2O_3, CaO, MgO, MnO, and ZrO_2. The Pd/HCM catalyst contains the PdO also in addition of these compounds which confirms the impregnation of Pd on HCMs.

The specific surface area of the prepared catalyst was calculated by NOVA touch 1F with nitrogen adsorption-desorption technique using BET surface area analyzer. The following equation was used to estimate the BET surface area.

$$\frac{1}{W\left(\frac{P}{P_0}-1\right)}=\frac{(C-1)}{W_mC}\left(\frac{P}{P_0}\right)+\frac{1}{W_mC} \tag{16}$$

Where P/P_0 is the relative pressure obtained from BET analysis; W_m, the weight of adsorbate as a monolayer (g); C, the BET constant; W, the weight of the adsorbed gas (cc/mol). The weight of the adsorbed gas, W can be determined using the volume of gas adsorbed as:

$$W=\frac{V\times M_w}{22.4\times 1000} \tag{17}$$

Where M_w is the molecular weight of the adsorbent gas (28.0134 g/ mol for Nitrogen) and V being the volume of adsorbed gas (cc/g). The relative pressure (P/P_0) and volume of gas adsorbed at STP calculated from equations (16) and (17) is presented in Table 2. Using the BET equation, by plotting $\left(\frac{P}{P_0}\right)$ vs $\frac{1}{W\left(\frac{P}{P_0}-1\right)}$ as shown in Fig. 5, provides a straight line having slope (S) $\frac{(C-1)}{W_mC}$ and intercept (i) of $\frac{1}{W_mC}$. W_m and C can be estimated. The value of W_m and C was obtained as 3.83×10^{-3} and 36.39 respectively. The total surface area (m^2) was estimated as:

$$S_t=\frac{W_mN_{av}A_{cs}}{\text{Molecular Weight of adsorbate}} \tag{18}$$

Where, N_{av} is Avogadro's number $=6.023\times10^{23}$ (mol); $A_{cs,}$ is adsorbate cross sectional area (16.2 Å2/mol for nitrogen). The specific surface area, (S_p) can be estimated as:

$$S_P=\frac{S_t}{W_s} \tag{19}$$

where W_s is the weight of the sample (g). The specific surface area calculated by Equation (19) was found to be 302.16 m^2/g.

The Fourier Transform Infrared Spectrum (FTIR) of the HCMs support and Pd supported on HCMs catalyst was done using Shimadzu Corporation IR Affinity-1 (Japan). The range of the IR spectrum varies from 4000 to 400 cm^{-1}. The different types of functional groups were detected by plotting the percent transmission versus wavenumber. FTIR analysis for bare HCM support was performed within the range 4000 to 400 cm^{-1}

Table 2
Relative pressure (P/P_0) and volume of gas adsorbed at STP.

Relative Pressure (P/P_0)	Volume Adsorbed (cc/g)	Weight of Adsorbent (g)	$1/[W(P/Po-1)]$
0.050	2.24561	0.0028	18.88
0.110	2.73455	0.0034	36.31
0.173	3.21443	0.0040	52.05
0.234	3.67896	0.0046	66.71
0.297	4.10366	0.0051	82.38

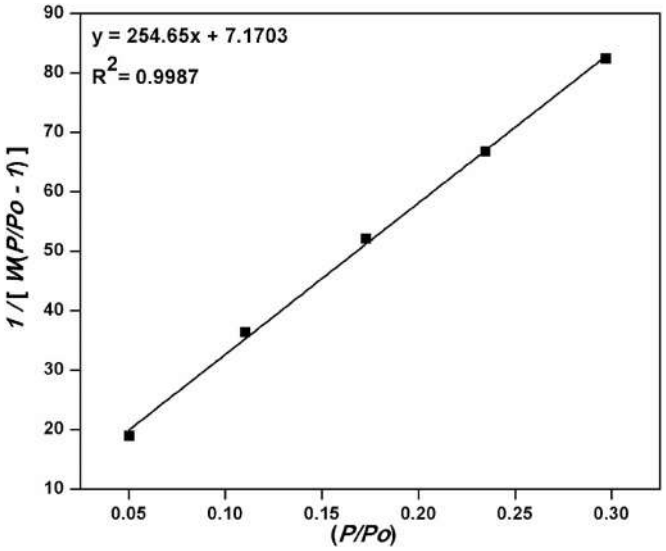

Fig. 5. N_2 adsorption isotherm using Pd/HCM catalyst.

(Fig. 6a). Broad bands at 3653-3556 cm^{-1} indicate linkage of oxygen to hydrogen (OH) bonds. The broad band at 1578-935 cm^{-1} shows asymmetric vibrations [35,36]. The intensities for pore openings which are at wavenumbers lower than 400 $cm^{-1}$are quite less. The bending vibrations for the water molecules could not also be detected, during the detailed FTIR study aimed at investigating the role of the support in promoting the production of hydrogen peroxide over Pd/HCM catalyst. Fig. 6b represents the plot of percent transmission vs wavenumber to analyze the functional group for further confirmation of Pd metal. Fig. 6b, shows the IR spectrum of Pd/HCM catalyst and the broad band present at 1085 cm^{-1} corresponds to Si–O–Si stretching vibrations [37]. The FTIR spectrum of the catalyst after the hydrogenation reaction is presented in Fig. 6c. The band absorptions at various positions, particularly at 1622, 2860, and 3433 cm^{-1}. The absorbtion band at 1622 cm^{-1} is due to asymmetric stretching of the Si–O–Si band. The IR spectrum of the used catalyst shows a broad intense band at 3433 cm^{-1} due to hydroxyl groups on the catalyst surface whereas the peak at 2860 cm^{-1}can be attributed to bending mode (δ O–H).

It can be concluded that the addition of H_2O_2 (25%) and $NH_3{\cdot}H_2O$ (30%) introduce the oxygen-containing functional groups onto the surface of the HCMs. The oxidation state of the metallic phase was achieved by heat treatment. The metal phase on the fresh virgin catalyst (without heat treatment) was primarily in metallic form (Pd^0). After heat treatment by calcination, palladium oxide (PdO) could be found, and the amount of PdO increases with increase in temperature. However, the

Table 1
The compositions of HCMs support and Pd/HCM catalyst.

Compound	Al_2O_3	SiO_2	Fe_2O_3	CaO	MgO	PdO	MnO	ZrO_2
HCM	35.709%	53.813%	4.172%	0.874%	5.528%	–	220.7ppm	393.2ppm
Pd/HCM	22.548%	31.209%	3.364%	0.701%	5.279%	0.422%	200.5ppm	533.1ppm

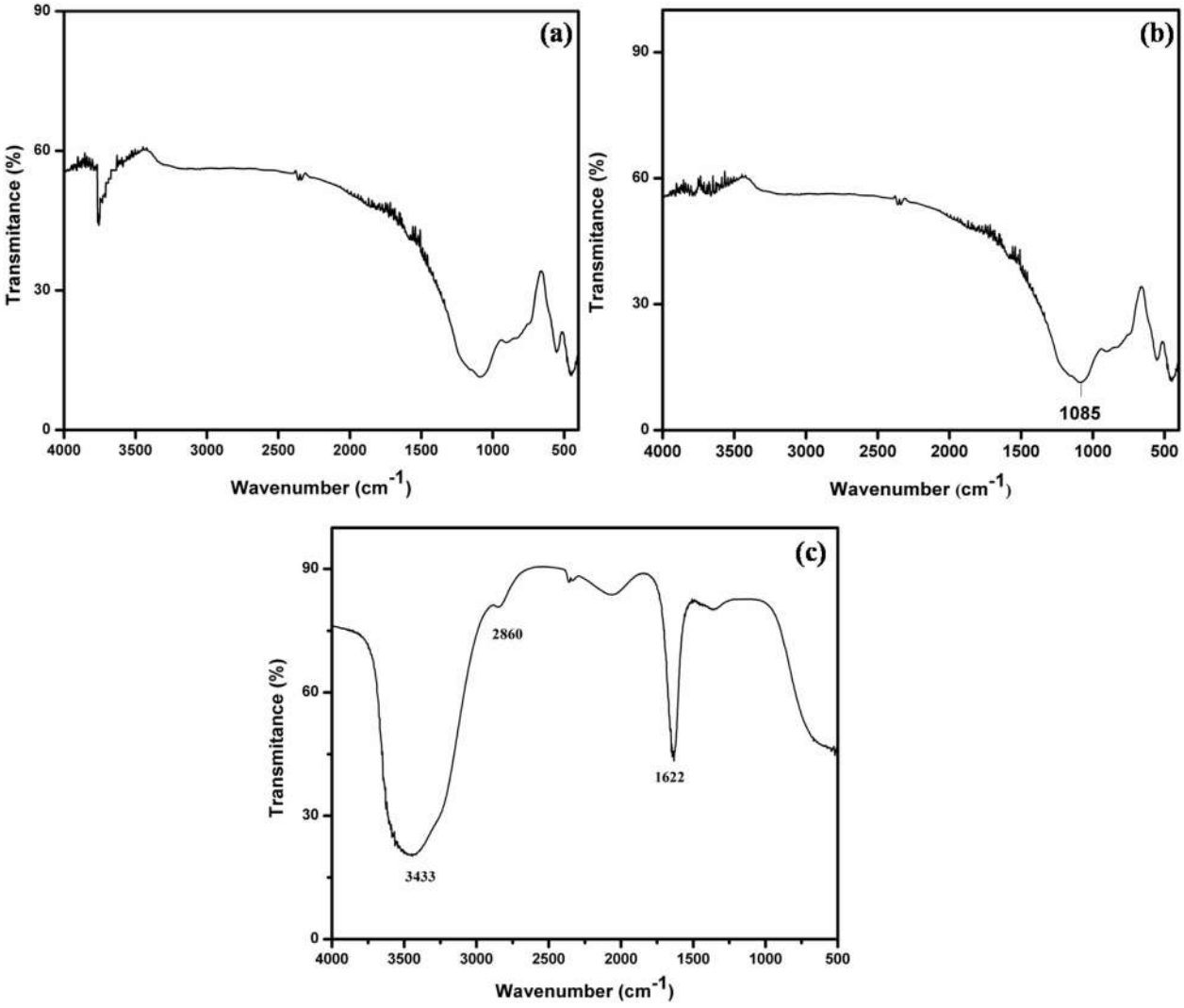

Fig. 6. FTIR spectrum of (a) HCMs support, (b) Pd/HCM catalyst, and (c) Pd/HCM catalyst after the hydrogenation reaction.

heat treatment by reduction does not lead to the formation of PdO but damages the oxygen-containing functional groups on the surface of the support.

3.2. Test for catalyst activity

3.2.1. Effect of reaction time

Catalytic hydrogenation experiments were performed to observe reaction kinetics of EAQ hydrogenation with respect to reaction time by varying the time from 0.5 to 2.66 h with initial EAQ concentration of 109 g/L at 75°C and 0.3 MPa in a high pressure autoclave reactor by using a Pd/HCM catalysts. Hydrogenation reaction of EAQ over supported Pd catalyst is zero order with respect to EAQ [18]. To understand the progress of the reaction with respect to time, the effect of reaction time on the yield of H_2O_2 and conversion of EAQ was investigated (Fig. 7). The volume of working solution and amount of catalyst was kept constant at 30 mL and 26.66 g/L respectively. The time of hydrogenation reaction plays a vital role in the hydrogenation process. It was observed from Fig. 7, that the yield of H_2O_2 and the conversion of EAQ both was found to be increased with an increase in the reaction time from 0.5 to 2.66 h.

Plot of conversion of EAQ per unit time was estimated to know the values of the rate constant using integral method of analysis (Eq. (1)). According to integral method, Eq. (1) can be rewritten as:

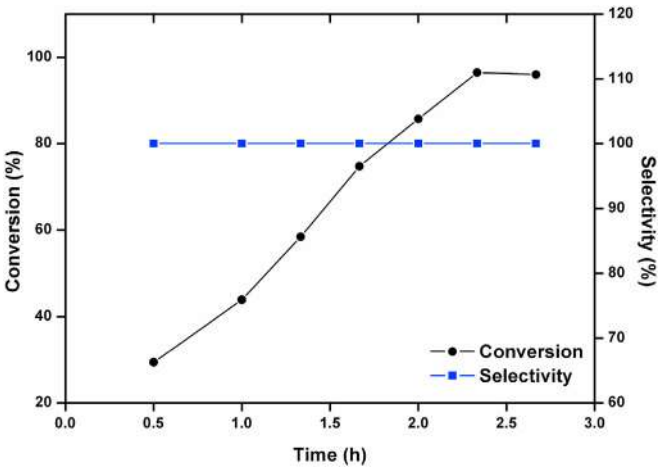

Fig. 7. Effect of reaction time on the conversion of EAQ and selectivity (Reaction conditions: Working solution volume = 30 mL, temperature = 75°C, pressure = 0.3 MPa, initial concentration of EAQ = 109 g/L, catalyst dose = 26.66 g/L).

$$C_{EAQ_0} - C_{EAQ} = C_{EAQ_0} x_{EAQ} = kt \quad (20)$$

The rate constant k can be obtained from a plot of (x_{EAQ}) against reaction time (t) yield a straight line passing through origin with slope k is equal to 169.2×10^{-3} m^3/kg·s.The plot of concentration of EAQ vs. time suggests the following of zero order kinetics in respect of the concentration of EAQ (Fig. 8). Hence it is confirmed that the hydrogenation reaction over as prepared catalyst (Pd/HCM) follows zero order for EAQ concentration.

The rate of hydrogenation over Pd/HCM catalyst for the conversion of EAQ (r_{EAQ}), formation of the EAHQ (r_{EAHQ}), and the consumption of H_2(r_{H_2}) were investigated for the reaction time and amounts of catalyst. The slope of the plots of the concentrations of reactant and product per unit time were estimated to obtain the values of the rates of r_{EAQ}, and r_{EAHQ}. The rate of conversion of EAQ was almost constant until $x = 60\%$ at a low catalyst amount (Fig. 9a) for 6.66 g/L of catalyst. Whereas it sharply decreases at higher conversions. r_{EAHQ}, was also found to be constant under the same conditions (6.66 g/L and 10 g/L of catalyst). The r_{EAHQ} was found to be directly proportional to r_{EAQ} and r_{H_2}. The r_{EAHQ} reaches a maximum value at higher amounts of catalyst whereas it reduces over the entire reaction period at higher conversion as shown in Fig. 9b and c. r_{EAHQ} reduced.The hydrogenation reaction of EAQ over Pd/HCM catalyst is a zero-order in regard of EAQ concentration and first order with respect to H_2 concentration (According to the integral method of analysis). For zero order reaction, the rate of reaction is equals to the rate constant and it is constant over the entire period of reaction. Hence in Fig. 9, the rate of conversion of EAQ is almost constant throughout the reaction for all catalyst doses.

For first order reaction, the rate of reaction is decreases as the concentration of H_2 falls in the reaction as H_2 is being consumed in the reaction. Hence in Fig. 9, the rate of H_2 consumption is decreases with reaction time. As the overall order of the reaction is became first order hence the rate of formation of the EAHQ is also decreasing in the Fig. 9.The nature of the kinetic curves was similar at 6.66 26.66 g/L of the catalyst dosages as shown in Fig. 9a, b, and c. Also, it is observed that the nature of the kinetic curves does not change with increasing the catalyst dosages.

3.2.2. *Effect of hydrogen pressure*

The catalytic activity of both Pd/Al_2O_3 and Pd/HCM catalysts increases constantly with an increase in EAQ concentrations and it can be confirmed from the development of the kinetic rate model. It was observed from the effect of varying the concentration of EAQ on the reaction rate. Fig. 10 describes nearly zero order dependency of conversion of EAQ on the concentration of EAQ. The rate of reaction for hydrogen in the liquid-phasehydrogenation reaction of EAQ was evaluated by considering the concentration of consumed hydrogen. Hence, the experiments were conducted to study the effect of varying H_2 pressure on the EAQ hydrogenation. Fig. 11 shows the EAQ conversions using both Pd/Al_2O_3 and Pd/HCM catalysts increase with the H_2 pressure, indicating the apparent reaction orders for H_2 follows almost first order using both Pd/Al_2O_3 and Pd/HCM catalysts.

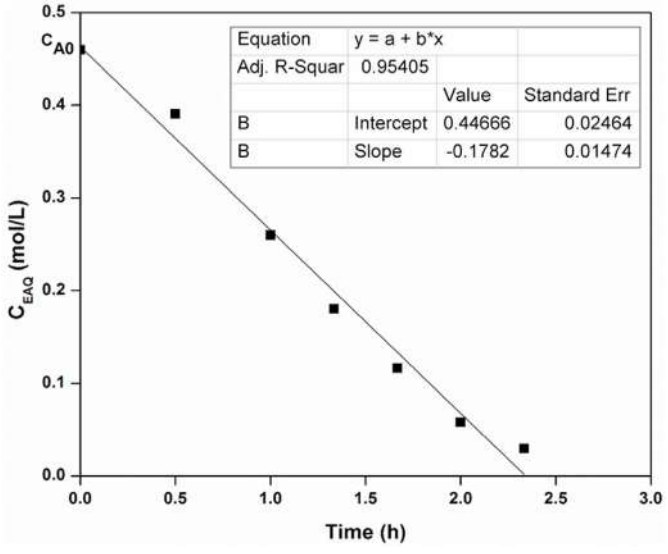

Fig. 8. The rate of change of EAQ over kinetic catalyst (Reaction conditions: Temperature = 75°C, pressure = 0.3 MPa, catalyst dose = 0.8 g, initial EAQ concentration = 109 g/L, working solution volume = 30 mL).

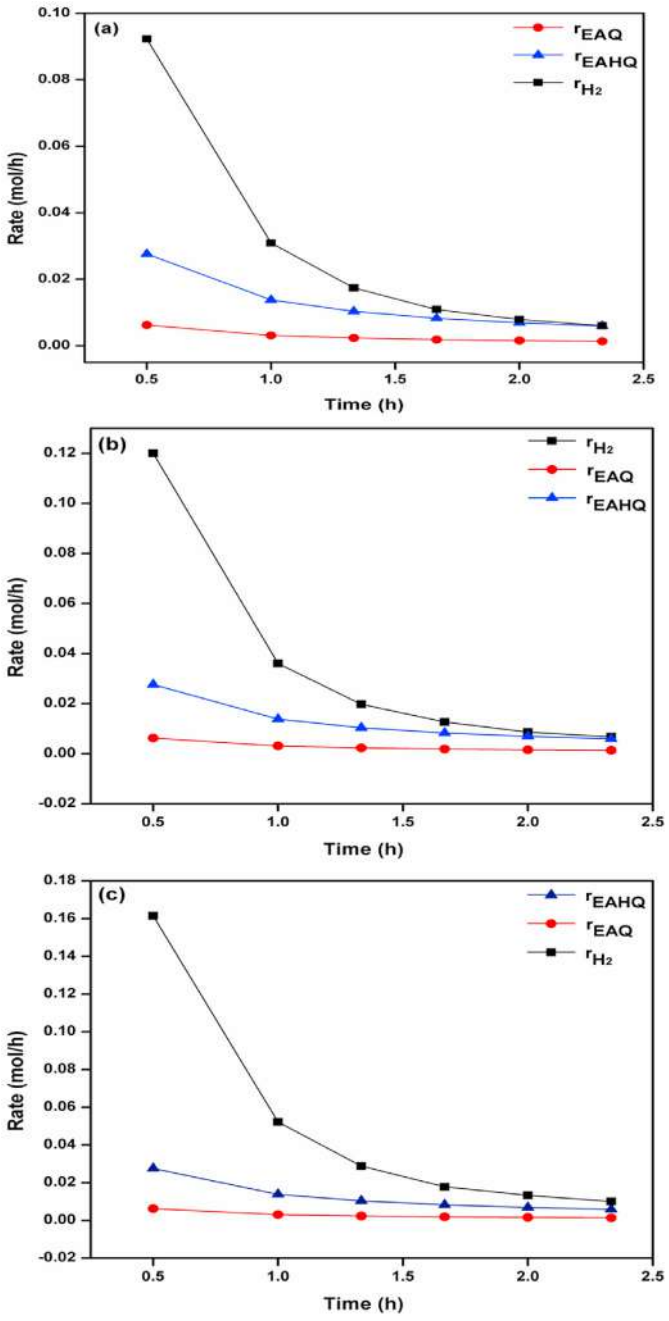

Fig. 9. The rates of EAQ conversion, EAHQ formation and hydrogen consumption as a function of reaction time (Reaction conditions: Temperature = 75°C, pressure = 0.3 MPa, initial concentration of EAQ = 109 g/L, volume of WS = 30 mL, and catalyst doses (a) 6.66 g/L, (b) 16.67 g, (c) 26.66 g/L.

3.2.3. *Effect of reaction temperature*

The kinetics of hydrogenation of EAQ, the effects of reaction tem-

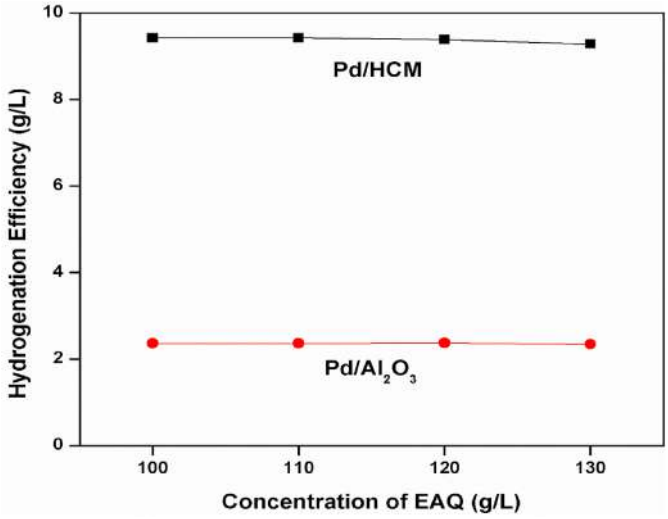

Fig. 10. Effect of EAQ concentration on the hydrogenation efficiency (Reaction conditions: H_2 pressure = 0.1–0.4 MPa, stirring speed = 1000 rpm, catalyst dose = 26.66 g/L, temperature = 75°C, time = 2.33 h).

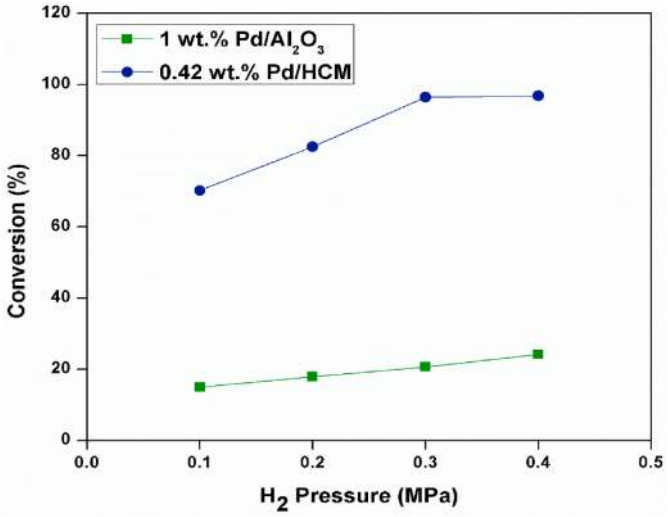

Fig. 11. Conversion of EAQ as a function hydrogen pressure (Reaction conditions: Temperature = 75°C, catalyst dose = 26.66 g/L, time = 2.33 h).

peratures on the yield of H_2O_2, and the conversion of EAQ were studied. In this study, the reaction was held at different temperatures from 50 to 75°C (Fig. 12). The reaction parameters were fixed at 30 mL of the volume of the working solution and 26.66 g/L of catalyst amount. The temperature of the hydrogenation reaction plays a significant role in the hydrogenation process. It has been found that the yield of H_2O_2 and the conversion of EAQ both increase extensively with increasing in the reaction temperature. The correlation between the yield and reaction time is as follows:

$$\ln(1/(1-y)) = kt \tag{21}$$

The plot of ln(1/(1-*y*)) and reaction time (*t*) is shown in Fig. 13. A linear relationship was found between the yield and reaction time. Each fitting line were obtained R^2 value as 0.965, 0.970, 0.949 and 0.962 with the respective slopes of 0.276, 0.354, 0.911 and 1.346 at various temperatures of 50°C, 6°C, 70°C and 75°C respectively. From the linearity of the plot (Fig. 13), it can be concluded that the hydrogenation reaction obeys zero order and first-order kinetics in respect of the concentration of EAQ and H_2 using Pd/HCM catalyst [18].

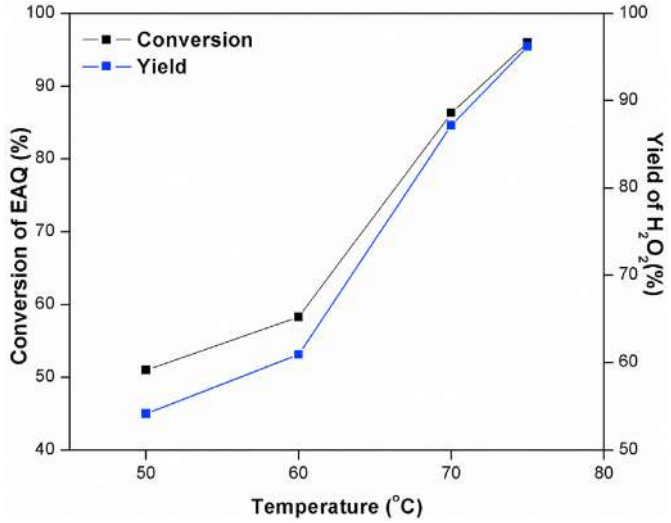

Fig. 12. Conversion of EAQ and Yield of H_2O_2 as a function of reaction temperature (Reaction conditions: Working solution volume = 30 mL, temperature = 75°C, pressure = 0.3 MPa, initial concentration of EAQ = 109 g/L, catalyst amount = 26.66 g/L).

The calculation of activation energy was attempted using the Arrhenius equation as shown in equation (14). The plot of ln*k* and 1/*T* was found to be linear as shown in Fig. 14 with the R^2value of 0.989. The activation energy was found to be 55.893 kJ/mol and can be expressed with the relation:

$$\ln k = lnk_0 - \frac{E}{RT} \tag{22}$$

3.2.4. *Effect of volume of working solution*

The effect of the volume of working solution on the yield of H_2O_2 and the conversion of EAQ is elaborated in Fig. 15. It was found that the highest conversion of EAQ and the yield of H_2O_2 could be achieved at 30 mL of the volume of the working solution. The gas-liquid interfaces and the catalyst amount can be correlated with the volume of the working solution. If one of the parameters is changed, the volume of the working solution changes significantly. The reaction is found to be hampered with the formation of degradation products at less volume of working solution (20 mL) due to less amount of EAQ present into the reactor and consequently, it lowers down the conversion of EAQ as well as yield of H_2O_2. However, when the volume of the working solution increases to a higher value (40 mL), both the conversion and the yield of H_2O_2 decrease simultaneously. It was found that the volume of the working solution plays a critical role in the hydrogenation reaction and to be maintained optimally at 30 mL for the reaction using Pd/HCM catalyst at 75°C and 0.3 MPa.

3.2.5. *Effect of catalyst dosages*

The effect of catalyst dosages (6.66–26.66 g/L) on the hydrogenation efficiency was studied at the constant temperature of 75°C and the reaction time of 2.33 h with the initial concentration of EAQ as 109 g/L. It was observed that the hydrogenation efficiency increases with the catalyst dosages [38]. It can be attributed to the availability of more active sites for the adsorption of EAQ on the surface of the catalyst. The hydrogenation efficiency was found to be 6.88 $g_{H_2O_2}$/L using the catalyst dose of 6.66 g/L which could enhance to 9.42 $g_{H_2O_2}$/Lusing 26.66 g/L of catalyst. The hydrogenation efficiency was not changed considerably with further increase in catalyst dosages. The comparison of the performance of Pd/HCM catalyst with conventional catalyst (Pd/Al_2O_3) and bimetallic catalyst ($Pd–Ir/Al_2O_3$) are incorporated in Table 3 [39].

The superior performance of the hollow microporous structure of Pd/

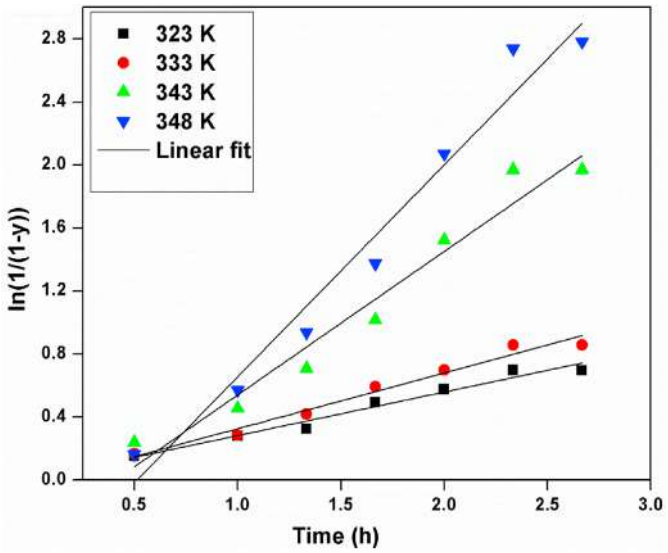

Fig. 13. Plot of $\ln(1/(1-y))$ vs. reaction time.

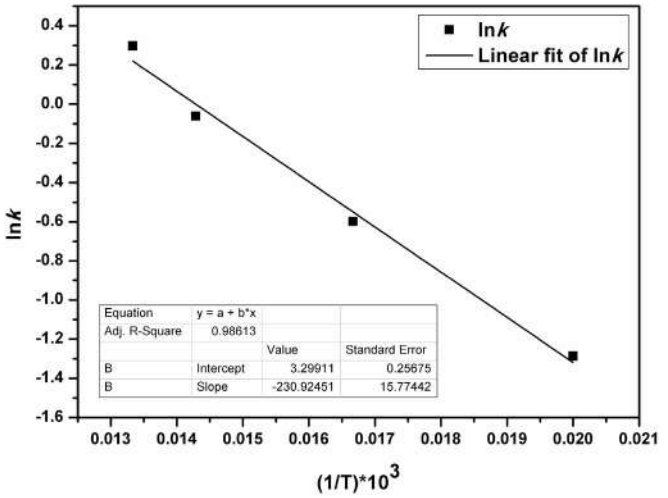

Fig. 14. Linear fitting of ln$k$ and $1/T$.

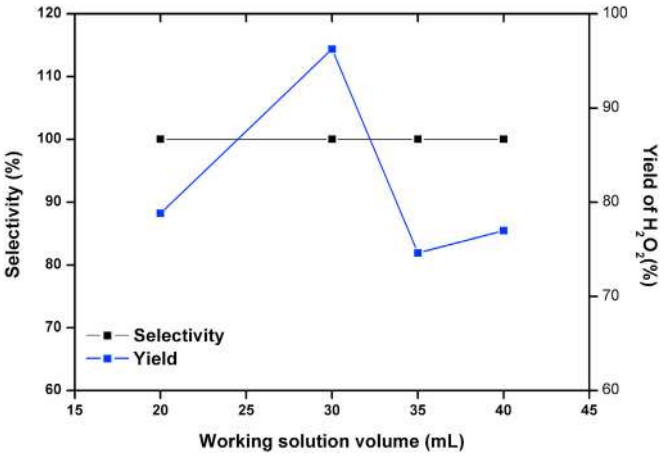

Fig. 15. The selectivity and yield of H_2O_2 as a function of working solution volume (Reaction conditions: Temperature = 75°C, pressure = 0.3 MPa, initial concentration of EAQ = 109 g/L, catalyst dose = 26.66 g/L).

Table 3
Performance of Pd/Al_2O_3, $Pd–Ir/Al_2O_3$ and Pd/HCM catalyst in the hydrogenation of EAQ.

Catalyst	Yield (%)	B (g/L)
Pd/HCM	96.4	9.4
$Pd–Ir/Al_2O_3$	92.1	3.2
Pd/Al_2O_3	61.0	2.5

HCM prepared catalyst can be proved with the Thiele modulus and effective internal diffusion factors for the hydrogenation reaction of EAQ eventually quantify the internal mass transfer resistance. In the mass transfer process of reactant H_2, the concentration gradients of H_2 can be determined by the concentration of H_2 in the gaseous phase, gas-liquid interface, and liquid phase according to the two-film theory [11]. The kinetic model for the reaction of EAQ hydrogenation would be expressed as equation (1) which can also be written as

$$r_{EAQ} = -\frac{dC_{EAQ}}{dt} = K^* C_{H_2} \tag{23}$$

in which the apparent reaction rate constant K^* can be dependent on hydrogen transportation resistances composing gas film resistance, gas-liquid film resistance, liquid-solid interface resistance, and the intrinsic reaction rate.

Using equation (11) and from the plot of $1/r$ vs $1/m_s$ for stirring speed of 1000 rpm, the intercept, C_1' was found to be 0.03276 m^3s/mol for H_2 pressure of 3 atm and $1/m_s$ as equal to 2307.83 [33]. The mass transfer resistance can be calculated by substituting all in the equation (24) and found the gas-liquid mass transfer coefficient $k_{gl}a_{gl}$.as 13.045 1/s.

$$C_1' = \frac{H_r}{\left[k_{gl}a_{gl}\, P_{H_2}\right]} \tag{24}$$

The specific surface area can also be investigated from equation (10). Being m_s as catalyst loading, calculated as 0.0216 $kg_{catalyst}/kg_{liquid}$; dp, the catalyst particle diameter as 5×10^{-5} m; ρ_l, the density of EAQ as 1231 kg/m^3; and $\rho_p\rho_p$ is the catalyst density as 1500 kg/m^3. On substituting the values in equation (10), the value of the specific surface area was found to be 2127.168 $m^2_{catalyst}/m^3_{liquid}$.

The Thiele Modulus for the catalyst used in the study wasestimated using Equation (25) [33].

$$\varphi_s = L\sqrt{\frac{k\rho_p}{D_{eff}}} \tag{25}$$

where, L = R/3 = $dp/6$ = 8.33×10^{-6} m; Rate Constant, k = 169.2×10^{-3} $m^3/kg{\cdot}s$. The molecular diffusivity of H_2can be given by the relationshipas expressed in the equation (26) [40].

$$D_{H_2} = 1.05 \times 10^{-2} exp\left[\frac{-1520}{T}\right] \tag{26}$$

The reaction temperature, T = 75°C = 348 K, put in the above equation to find the the diffusivity of H_2 was found to be 0.0133×10^{-2} cm^2/s or 0.0133×10^{-6} m^2/s at the reaction temperature, T = 75°C = 348 K.

Using these estimated values in equation (25), the value of Thiele Modulus was found to be 0.0289.

Also, the effectiveness factor for the first order reaction w.r.t. H_2 for the above value of Thiele Modulus was calculated using equation (27) [33].

$$\eta_s = \frac{\tanh \varphi_s}{\varphi_s} \tag{27}$$

The value of effectiveness factor, η_s was found to be 1.0.

The intrinsic rate expression for the hydrogenation of EAQ obtained

in a stirred tank reactor excluding any mass transfer limitations suggested by Chen et al. can be represented as equation (28) [41]:

$$r_{H_2} = 0.9936 \times 10^{-8} exp\left(\frac{-17.041}{RT}\right) P_{H_2} \quad (28)$$

where R is Gas constant, as 8.314 J/mol·K; P_{H_2}, partial pressure of H_2, as 3 atm; T, the temperature of the reaction, as 348 K. Put all these values in the above equation to calculate the rate of reaction. On substituting all values in the above equation (26), the rate of reaction was found to be 9.935×10^{-9} mol/m^3·s.

Thus the rate of reaction enhances with the introduction of a supported Pd/HCM catalyst. The particle size and the dispersion of active metal on the surface of the catalyst support, are the most important parameters to improve the catalytic performance of the catalyst. The modified pore structure of the support increases the dispersion of Pd and decreases the diffusion resistance. Hence, the synthesized catalyst Pd supported on HCMs has provided higher catalyst activity at lower activation energy with less Pd loading amount (0.42 wt.%) as compared to conventional catalyst support. The conventional catalyst support Al_2O_3 used in the hydrogenation of anthraquinone compound shows a low yield of 61% and the hydrogenation efficiency of 2.34 g/L and the loss of active quinone compound. The use of HCMs as catalyst support increases the hydrogenation efficiency (9.42 g/L) and the yield of H_2O_2 (96%).

4. Conclusions

Pd/HCM catalyst was used to investigate the hydrogenation of EAQ at the catalyst doses ranging from 6.66 to 30 g/L. At 75°C and 0.3 MPa, the hydrogenation of an aromatic compound, EAQ using Pd/HCM catalyst could provide the high conversion (96%) with less EAQ consumption. The kinetic models of the heterogeneous reaction of EAQ with a Pd/HCM catalyst was also studied. The reaction follows the zero order and first order kinetics with respect to the concentration of EAQ and H_2 respectively. The shape of the kinetic curve was found to be altered with an increase in the catalyst dose. The heterogeneous system in the high-pressure autoclave reactor with a spherical catalyst had an effectiveness factor of 1.0. The three-phase chemical reaction was also been studied in the Gas-Liquid and Liquid-Solid mass transfer areas.

Declaration of competing interest

The authors declare that they have no known competing financial interestsor personal relationships that could have appeared to influence the work reported in this paper.

References

[1] Campos-Martin JM, Blanco-Brieva G, Fierro JLG. Hydrogen peroxide synthesis: an outlook beyond the anthraquinone process. Angew. Chem. Int. Ed. 2006;45:6962–84. https://doi.org/10.1002/anie.200503779.

[2] Cheng Y, Wang L, Lu S, Wang Y, Mi ZT. Gas-liquid-liquid three-phase reactive extraction for the hydrogen peroxide preparation by anthraquinone process. Ind. Eng. Chem. Res. 2008;47:7414–8. https://doi.org/10.1021/ie800500y.

[3] Liu G, Duan Y, Wang Y, Wang L, Mi ZT. Periodically operated trickle-bed reactor for EAQs hydrogenation: experiments and modeling. Chem. Sci. 2005;60:6270–8. https://doi.org/10.1016/j.ces.2005.03.028.

[4] Riedl HJ, Pfiefderer G. Production of hydrogen peroxide. IG farbenindustrie. Aktiengesellschaft frankfort-on-the-main, Germany. U.S. Patent. 1939;2(158):525.

[5] Hou Y, Wang Y, He F, Mi W, Mi Z, Wu W, Min E. Effects of lanthanum addition on Ni-B/γ-Al_2O_3 amorphous alloy catalysts used in anthraquinone hydrogenation. ApplCatal A: GEN 2004;259:35–40. https://doi.org/10.1016/j.apcata.2003.09.006.

[6] Liu B, Qiao M, Deng JF, Fan K, Zhang X, Zong B. Skeletal Ni catalyst prepared from a rapidly quenched Ni-Al alloy and its high selectivity in 2-ethylanthraquinone hydrogenation. J. Catal. 2001;204:512–5. https://doi.org/10.1006/jcat.2001.3405.

[7] Isaka Y, Yamada Y, Suenobu T, Nakagawa T, Fukuzumi S. Production of hydrogen peroxide by the combination of semiconductor-photocatalyzed oxidation of water and photocatalytic two-electron reduction of dioxygen. RSC Adv. 2016;6:42041–4. https://doi.org/10.1039/C6RA06814F.

[8] Freakley SJ, He Q, Harrhy JH, Lu L, Crole DA, Morgan DJ, Ntainjua EN, Edwards JK, Carley AF, Borisevich AY, et al. Palladium-tin catalysts for the direct synthesis of H_2O_2 with high selectivity. Science 2016;351:965–8. https://doi.org/10.1126/science.aad5705.

[9] Hong R, Feng J, He Y, Li D. Controllable preparation and catalytic performance of Pd/anodic alumina oxide@Al catalyst for hydrogenation of ethylanthraquinone. Chem. Sci. 2015;135:274–84. https://doi.org/10.1016/j.ces.2015.04.003.

[10] Li Y, Feng J, He Y, Evans DG, Li D. Controllable synthesis, structure, and catalytic activity of highly dispersed Pd catalyst supported on whisker-modified spherical alumina. Ind. Eng. Chem. Res. 2012;51:11083–90. https://doi.org/10.1021/ie300385h.

[11] Kosydar R, Drelinkiewicz A, Lalik E, Gurgul J. The role of alkali modifiers (Li, Na, K, Cs) in activity of 2% Pd/Al_2O_3 catalysts for 2-ethyl-9,10-anthraquione hydrogenation. ApplCatal A: GEN 2011;402:121–31. https://doi.org/10.1016/j.apcata.2011.05.036.

[12] Drelinkiewicz A, Laitinen R, Kangas R, Pursiainen J. ApplCatal A: GEN 2005;284:59–67. https://doi.org/10.1016/j.apcata.2005.01.018.

[13] Drelinkiewicz A, Waksmundzka-Gora A. Investigation of 2- ethylanthraquinone degradation on palladium catalysts. J. Mol. Catal. Chem. 2006;246:167–75. https://doi.org/10.1016/j.molcata.2005.10.026.

[14] Drelinkiewicz A. Deep hydrogenation of 2-ethylanthraquinone over Pd/SiO_2 catalyst in the liquid phase. J. Mol. Catal. 1992;75:321–32. https://doi.org/10.1016/0304-5102(92)80134-3.

[15] Drelinkiewicz A, Kangas R, Laitinen R, Pukkinen A, Pursiainen J. Hydrogenation of 2-ethylanthraquinone on alumina-supported palladium catalysts: the effect of support modification with Na_2SiO_3. ApplCatal A: GEN 2004;263:71–82. https://doi.org/10.1016/j.apcata.2003.12.010.

[16] Drelinkiewicz A, Pukkinen A, Kangas R, Laitinen R. Hydrogenation of 2-ethylanthraquinone over Pd/SiO2 and Pd/Al2O3 in the fixed-bed reactor. The effect of the type of support. Catal Lett 2004;94:157–70. https://doi.org/10.1023/BCATL.0000020540.90536.6d.

[17] Guo Y, Dai C, Lei Z. Hydrogenation of 2-ethylanthraquinone with monolithic catalysts: an experimental and modelling study. Chem. Sci. 2017;172:370–84. https://doi.org/10.1016/j.ces.2017.06.032.

[18] Santacesaria E, Di-Serio M, Russo A, Leone U, Velotti R. Kinetic and catalytic aspects in the hydrogen peroxide production via anthraquinone. Chem. Sci. 1999;54:2799–806. https://doi.org/10.1016/S0009-2509(98)00377-7.

[19] Hu H, Liu B, Qiao M, Fan K, He H. Selective hydrogenation of 2-ethylanthraquinone over an environmentally benign Ni-B/SBA-15 catalyst prepared by a novel reductant–impregnation method. J. Catal. 2003;220:254–7. https://doi.org/10.1016/j.jcat.2003.07.007.

[20] Fang J, Chen X, Liu B, Yan S, Qiao M, Li H, He H, Fan K. Liquid-phase chemoselective hydrogenation of 2-ethylanthraquinone over chromium-modified nanosized amorphous Ni–B catalysts. J. Catal. 2005;229:97–104. https://doi.org/10.1016/j.jcat.2004.10.014.

[21] Wang F, Xu X, Sun K. Hydrogenation of 2-ethylanthraquinone over Pd/ZrO_2-γ-Al_2O_3 catalyst. React KinetCatal Lett 2008;93:135–40. https://doi.org/10.1007/s11144-008-5218-5.

[22] Shen C, Wang YJ, Xu JH, Lu YC, Luo GS. Preparation and the hydrogenation performance of novel catalyst-Pd nanoparticles loaded on glass beads with an egg–shell structure. Chem. Eng. J 2011;173:226–32. https://doi.org/10.1016/j.cej.2011.07.025.

[23] Shang H, Zhou H, Zhu Z, Zhang W. Study on the new hydrogenation catalyst and processes for hydrogen peroxide through anthraquinone route. J. Ind. Eng. Chem. 2012;18:1851–7. https://doi.org/10.1016/j.jiec.2012.04.017.

[24] Tang P, Chai Y, Feng J, Feng Y, Li Y, Li D. Highly dispersed Pd catalyst for anthraquinone hydrogenation supported on alumina derived from a pseudo-boehmite precursor. ApplCatal A: GEN 2014;469:312–9. https://doi.org/10.1016/j.apcata.2013.10.008.

[25] Chen H, Huang D, Su X, Huang J, Jing X, Dub M, Sun D, Jia L, Li Q. Fabrication of Pd/γ-Al_2O_3 catalysts for hydrogenation of 2-ethyl-9,10-anthraquinone assisted by plant-mediated strategy. Chem. Eng. J 2015;262:356–63. https://doi.org/10.1016/j.cej.2014.09.117.

[26] Halder R, Lawal A. Experimental studies on hydrogenation of anthraquinone derivative in a microreactor. Catal. Today 2007;125:48–55. https://doi.org/10.1016/j.cattod.2007.03.055.

[27] Zang J, Li D, Zhao Y, Kong Q, Wang S. A Pd/Al_2O_3/cordierite monolithic catalyst for hydrogenation of 2-ethylanthraquinone. Catal. Commun. 2008;9:2565–9. https://doi.org/10.1016/j.catcom.2008.07.012.

[28] Liu B, Qiao M, Wang J, Fan K. Highly selective amorphous Ni-Cr-B catalyst in 2-ethylanthraquinone hydrogenation to 2- ethylanthrahydroquinone. Chem. Commun. 2002:1236–7. https://doi.org/10.1039/B202499N.

[29] Drelinkiewicz A, Waksmundzka-Gora A, Makowski W, Stejskal J. Pd/polyaniline(SiO_2) a novel catalyst for the hydrogenation of 2-ethylanthraquinone. Catal. Commun. 2005;6:347–56. https://doi.org/10.1016/j.catcom.2005.02.009.

[30] Drelinkiewicz A, Waksmundzka-Gora A. Hydrogenation of 2-ethyl-9,10-anthraquinone on Pd/SiO_2 catalysts: the role of humidity in the transformation of hydroquinone form. J Mol CatalA:Chem. 2006;258:1–9. https://doi.org/10.1016/j.molcata.2006.05.003.

[31] Drelinkiewicz A, Waksmundzka-Gora A, Sobczak JW, Stejskal J. Hydrogenation of 2-ethyl-9,10-anthraquinone on Pd-polyanaline (SiO_2) composite catalyst the effect of humidity. ApplCatal A: GEN 2007;333:219–28. https://doi.org/10.1016/j.apcata.2007.09.011.

[32] Levenspiel O. Chemical Reaction Engineering. third ed. New York: Wiley; 1972.

[33] Farrauto RJ, Bartholomew CH. Fundamentals of Industrial Catalytic Processes, vol. 46. Blackie Academic and Professional; 1998. p. 496–504.

[34] Ingle AA, Ansari SZ, Shende DZ, Wasewar KL, Pandit AB. Hydrogenation of 2-ethylanthraquinone with Pd supported on hollow ceramic microsphere catalyst: an

experimental and kinetic study. J. Indian Chem. Soc. 2020a;97:1033–7 [Accessed 2020 June 8]: [5 pp.].
[35] Li C, Wu Z. Microporous Materials Characterized by Vibrational Spectroscopies", Chinese Academy of Sciences. Dalian: China Marcel Dekker, Inc; 2003. p. 423–513. 2003.
[36] Ojha K, Pradhan NC, Samanta AN. Zeolite from fly ash: synthesis and characterization. Bull. Mater. Sci. 2004;27:555–64.
[37] Dhokte A, Sonkamble S, Lande M, Arbad B. One-pot synthesis of aromatic nitriles from aldehydes using magnetic material separated from coal fly ash. IJCPS 2014;5: 75–81.
[38] Ingle AA, Ansari SZ, Shende DZ, Wasewar KL, Pandit AB. Palladium supported on nano-hybrid Zr–Al–La catalyst for hydrogenation of 2-ethylanthraquinone. Indian Chem Eng.; 2020b. https://doi.org/10.1080/00194506.2020.1749141 [Accessed 2020 April 8]: [15 pp.].
[39] Hong R, He Y, Feng J, Li D. Fabrication of supported Pd-Ir/Al2O3 bimetallic catalysts for 2-ethylanthraquinone hydrogenation. AIChE J. 2017;63:3955–65. https://doi.org/10.1002/aic.15748.
[40] Santacesaria E, Di Serio M, Velotti R, Leone U. Kinetics, mass transfer and palladium catalyst deactivation in the hydrogenation. IndEnggChem Res 1994;33:277–84. https://doi.org/10.1021/ie00026a016.
[41] Chen Q. Reviews on the hydrogenation kinetics for the preparation of hydrogen peroxide by anthraquinone process. InorgChem Ind 2001;33:20–2.